Bigleaf Maple Within-Crown Leaf Morphology and Seasonal Physiology

Article *in* Northwest Science · November 2020

DOI: 10.3955/046.094.0207

3 authors, including:

Lucy Kerhoulas
Humboldt State University
25 PUBLICATIONS **326** CITATIONS

SEE PROFILE

Nicholas Kerhoulas
Cal Poly Humboldt
8 PUBLICATIONS **126** CITATIONS

SEE PROFILE

Lucy P. Kerhoulas[1] and **David T. Hammons**, Department of Forestry and Wildland Resources, Humboldt State University, 1 Harpst Street, Arcata, California 95521

and

Nicholas J. Kerhoulas, Department of Wildlife, Humboldt State University, 1 Harpst Street, Arcata, California 95521

Bigleaf Maple Within-Crown Leaf Morphology and Seasonal Physiology

Abstract

We investigated the influences of height, light availability, leaf structure, and season on bigleaf maple (*Acer macrophyllum* Pursh) leaf physiology in northern California to improve our understanding of productivity and carbon sequestration in western forests. Using hydrated cuttings and lab-based measurements, we found that leaf mass-to-area ratio and maximum photosynthetic capacity increased with height and distance from the bole. *In situ*, we measured leaf physiology throughout tree crowns from June through September and found that predawn water potential was remarkably constant, indicating sustained access to water. We also found that midday water potential generally decreased with height and distance from the bole, noticeably decreased at the end of the growing season, and did not fall below –2 MPa, suggesting ample access to water and/or stomatal regulation to maintain hydrated water status. At midday, light availability and stomatal conductance of water vapor generally increased with height and distance from the bole. Stomatal conductance peaked in the treetop in June, in the mid-crown in July and August, and in the low-crown in September, demonstrating temporal and spatial optimization of crown resources in response to changing light quality, climatic conditions, and water status across the season to maximize carbon uptake at the tree level. Together, our water potential and light measurements suggest that light availability is a stronger determinant of leaf morphology and physiology than hydraulic limitation in this species. These findings provide information on seasonal physiology in a widespread deciduous hardwood species, thereby strengthening our understanding of forest productivity in a predominantly coniferous region.

Keywords: dark respiration, hardwood, maximum photosynthesis, stomatal conductance, water potential

Introduction

Hardwood broadleaved tree species are important components of western North American forests, often having higher leaf-level photosynthetic and carbon sequestration rates than co-occurring conifers (Rhemtulla et al. 2009). In deciduous species, physiology can vary seasonally throughout the annual leaf lifespan, although few studies have tried to quantify intra-annual trends in hardwood productivity. Leaf structure and physiology can also vary spatially within tree crowns due to differences in the gravitational component of water potential (Ψ) and light availability (Mullin et al. 2009). Compared to shade leaves and leaves from the low crown, sun leaves generally have thicker palisade layers, resulting in higher leaf mass-to-area ratios (LMA), maximum photosynthetic rates (A_{max}), and dark respiration rates (R_{dark}) (Lichtenthaler et al. 1981). *In situ*, greater light exposure in the upper and outer crown typically increases gas exchange capacity in sun leaves such that transpirational water loss is also correspondingly greater in these crown regions (Catoni et al. 2015). As such, stomatal regulation to conserve water may become a limiting factor to productivity in sun leaves, particularly as water availability decreases throughout the growing season in climates with dry summers.

While within-crown structural and physiological differences between sun and shade leaves have been documented for some species, the predominant drivers of these gradients are still unclear for many species. In tall (> 100 m) redwood (*Sequoia sempervirens* (D. Don) Endl.) trees, the gravitational component of water potential appears to be the primary determinant of leaf structure (Oldham

[1]Author to whom correspondence should be addressed.
Email: lucy.kerhoulas@humboldt.edu

et al. 2010) and resulting physiology (Mullin et al. 2009), while in tall Sitka spruce (*Picea sitchensis* (Bong.) Carr.) trees, light appears to be the primary determinant (Chin and Sillett 2017, Kerhoulas et al. 2020). In tall conifers, hydrostatic tension in the water column increases with height due to gravity, making it difficult for cells to maintain turgor and elongate; these conditions produce leaf mesophylls densely packed with small cells (Koch et al. 2004, Woodruff et al. 2004). Low mesoporosity in treetop foliage can reduce photosynthetic capacity despite greater exposure to light by increasing R_{dark} and decreasing internal CO_2 conductance (g_i) (Mullin et al. 2009). In the conifer-dominated western United States, relatively little research has been done on within-crown variation in leaf structure and physiology in broadleaved species. It is therefore important to better understand temporal and spatial productivity patterns in western deciduous hardwoods to improve estimates of forest productivity and carbon sequestration, particularly as some research suggests a possible vegetation shift towards hardwood species in response to climate change and altered fire regimes (Sohngen and Brown 2006).

Given the need to improve our understanding of productivity patterns in western hardwoods, the objective of this study was to quantify leaf morphology and physiology within hardwood crowns across the growing season. For this investigation, we used bigleaf maple (*Acer macrophyllum* Pursh), as it is a ubiquitous deciduous hardwood species on the west coast of the United States, ranging from Alaska south through California (Stuart and Sawyer 2001). More specifically, to evaluate spatial trends in morphology and resulting physiological capacities, we made lab-based measurements of LMA, A_{max}, standardized maximum photosynthetic rate (A_{std}), R_{dark}, light saturation and compensation points (LSP and LCP, respectively), and g_i rates on mature leaves from hydrated cuttings (Table 1). To evaluate spatial and temporal physiological trends as they relate to leaf structure and within-crown microclimates, we made *in situ* measurements of light availability, stomatal conductance of water vapor (g_s, positively correlated with photosynthesis), predawn leaf water potential (Ψ_{PD}), and midday leaf water potential (Ψ_{MD}) across the growing season. We hypothesized the following: 1) LMA will increase with height and distance from the bole due to increasing light availability and hydrostatic tension; 2) due to increased LMA and associated changes in leaf structure (e.g., increased mesophyll density), leaves from the upper and outer crown will have decreased physiological capacity under optimal conditions, as reflected by reduced A_{max}, A_{std}, LSP, and g_i and increased R_{dark} and LCP; 3) Ψ_{PD} will decrease with height due to gravity, while Ψ_{MD} will decrease with height due to gravity and increasing light availability with height and distance from the bole; 4) increasing light availability will cause g_s to increase with height and distance from the bole, despite gravitational reductions in Ψ; and 5) across the growing season, light availability will peak in the middle (July/August), g_s will peak in the middle due to leaf phenology and residual winter water availability, and Ψ_{PD} and Ψ_{MD} will decrease as winter water inputs decrease and atmospheric vapor pressure deficit (VPD) increases.

Methods

Study Site and Study Trees

Our study occurred at the L.W. Schatz Demonstration Tree Farm in Maple Creek, California. This site is located at 160 m elevation, approximately 27 km from the Pacific Ocean. Overstory species in this forest include Douglas-fir (*Pseudotsuga menziesii* Franco), tanoak (*Notholithocarpus densiflorus* Manos), madrone (*Arbutus menziesii* Pursh), California bay (*Umbellularia californica* Nuttall), and bigleaf maple. This inland site is classified under the Köppen Climate Classification as "dry-summer subtropical," otherwise known as a Mediterranean climate. The site receives the majority of annual precipitation during the winter months and experiences hot, dry summers. Of the 164 cm of average annual rainfall, only 3 cm fall in the summer months. Maximum monthly temperature ranges annually between 19 and 39 °C (Weatherbase National Database 2019; Figure 1). We speculate that trees at this site thrive through the desiccating summer conditions by accessing deep water sources late in the growing season (Stone and Kalisz 1991), regulating stomatal

TABLE 1. Summary of terms and definitions used in this study.

Abbreviation	Definition	Units
$A_{max,a}$	Area-based maximum CO_2 assimilation rate	µmol CO_2 m^{-2} s^{-1}
$A_{max,m}$	Mass-based maximum CO_2 assimilation rate	nmol CO_2 g^{-1} s^{-1}
$A_{std,a}$	Area-based standardized CO_2 assimilation rate	µmol CO_2 m^{-2} s^{-1}
$A_{std,m}$	Mass-based standardized CO_2 assimilation rate	nmol CO_2 g^{-1} s^{-1}
C_i	Internal CO_2 concentration in substomatal chamber	µmol CO_2 mol^{-1}
$g_{i,a}$	Area-based internal CO_2 conductance rate	mol CO_2 m^{-2} s^{-1} bar^{-1}
$g_{i,m}$	Mass-based internal CO_2 conductance rate	nmol CO_2 g^{-1} s^{-1} bar^{-1}
g_s	Area-based stomatal CO_2 conductance rate	mmol CO_2 m^{-2} s^{-1}
LCP	Light compensation point	µmol photons m^{-2} s^{-1}
LMA	Leaf mass-to-area ratio	g m^{-2}
LSP	Light saturation point	µmol photons m^{-2} s^{-1}
$R_{dark,a}$	Area-based dark respiration rate	µmol CO_2 m^{-2} s^{-1}
$R_{dark,m}$	Mass-based dark respiration rate	nmol CO_2 g^{-1} s^{-1}
Ψ_{PD}	Predawn water potential	MPa
Ψ_{MD}	Midday water potential	MPa

conductance to minimize transpirational water loss and avoid embolisms (Davies and Kozlowski 1977), and perhaps supplementing soil water with water drip from fog and dew deposits (Ingraham and Matthews 1995).

We chose three large (approximately 30 m in height) bigleaf maples as our study trees. Each study tree was dominant and open grown with minimal competition for light. Using non-destructive arborist climbing techniques (Kramer et al. 2018), we sampled each study tree for morphology and physiology at six crown positions. We vertically stratified the crown into three height categories: low (4.0 ± 0.4 m), middle (14.2 ±1.5 m), and high (19.9 ± 1.6 m). Within each crown height category, we evaluated the lateral gradient by sampling from the inner and outer crown (relative to the bole).

Lab Measurements

To quantify within-crown morphological variation and the influence of these trends on leaf physiology, we used hydrated cuttings subjected to standardized conditions for lab-based measurements. In July (the middle of the May through October growing season) 2016, we cut two small branches (approximately 1 m length and 1 cm basal diameter) from each position in each tree. Branches were quickly recut under water, transported back to the Humboldt State University Forest Physiology Laboratory, and allowed to equilibrate overnight. Hydrated cuttings were kept in a glasshouse for up to three days; all measurements were taken during this time period. A more detailed description of how each parameter was calculated can be found in Mullin et al. (2009); below is a brief summary of our methods.

On each hydrated cutting ($n = 2$ per position per tree), we measured morphology and physiology. For LMA, a leaf was scanned (Epson America, Inc., Long Beach, CA) and Image J (National Institute of Health, Bethesda, MD) was used to measure leaf area; the leaf was then dried for 48 hours at 60 °C and weighed to determine mass. From each position in each tree, LMA was measured for five leaves and then averaged into a single value. Physiological measurements were made on a LiCor 6400 Portable Photosynthesis System (LiCor Biosciences, Lincoln, NE) equipped with a standard 2 × 3 cm leaf chamber and a red-blue LED light source. From each position, a light response curve and four CO_2 response curves were made. Whenever possible, the same leaf was used for all response curves; however, if between curves the leaf did not return to its baseline gas exchange rates, a new leaf was picked from the same cutting for subsequent curves. For each physiological

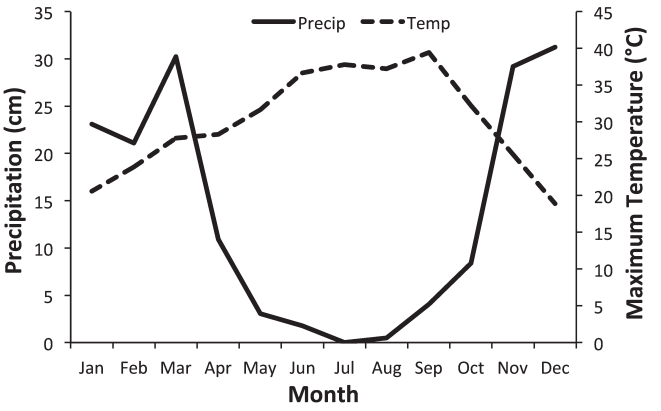

Figure 1. Monthly total precipitation (solid line) and maximum temperature (dashed line) at study site in Maple Creek, CA. Monthly values represent an average based on six years (2013–2018) of data (Weatherbase National Database 2019).

variable, values from the two cuttings per position were averaged into a single value.

For the light response curves, CO_2 was set to 400 ppm, temperature was held constant at 20 °C, vapor pressure deficit (VPD) was maintained at 1.24 ± 0.02 kPa, and light was set to the following sequence: 2000, 1600, 1200, 900, 600, 550, 400, 300, 200, 100, 50, 25, 0 μmol m^{-2} s^{-1}. From each light response curve, we calculated A_{max}, R_{dark}, LSP, LCP, and also recorded the internal CO_2 concentration (C_i) at which the highest photosynthetic rate was achieved. These A_{max} C_i values from each position on each tree were then averaged into a single value that was used with CO_2 response curves to calculate a standardized maximum photosynthetic rate (A_{std}, see below).

On each hydrated cutting, four CO_2 response curves were then made to calculate A_{std} and g_i. For the first CO_2 response curve, light was set to 1600 μmol m^{-2} s^{-1}, temperature was set to 20 °C, VPD was maintained at 1.21 ± 0.02 kPa, and CO_2 was set to the following sequence: 400, 250, 100, 50, 400, 600, 700, 900, 1200, 1600, 2000 ppm. Using the average A_{max} C_i value derived from the light curves, A_{std} was calculated for each cutting as the assimilation rate at this C_i value; this A_{std} value represents a standardized maximum photosynthetic capacity with both light and CO_2 levels held constant. Next, response curves were made at three light levels (1000, 200, 50 μmol m^{-2} s^{-1}) using the following CO_2 sequence of settings: 200, 100, 50, 25, 0 ppm; temperature was maintained at 20 °C, and VPD was maintained at 1.23 ± 0.02 kPa. These three CO_2 response curves were used to calculate g_i using the photocompensation point method (see Mullin et al. 2009 for more details).

In Situ Measurements

At each of the six crown positions on each study tree, *in situ* measurements of light, leaf Ψ (Ψ from here forward), and g_s were measured between June and September to understand the temporal influence of native conditions (e.g., light, temperature, relative humidity, and Ψ) on leaf morphology and physiology. At this study site, the authors observed that leaf emergence typically occurs in May and leaf senescence typically occurs in October; we therefore made *in situ* measurements in June, July, August, and September to ensure that we were measuring mature leaves that had not yet started autumn senescence. In September, although the very early stages of autumnal senescence were evident in the upper outer crown of our study trees, we only made *in situ* measurements on vibrantly green leaves. Only one tree was measured per sampling day because of the time required to complete the course of sampling. We measured light, Ψ, and g_s using a light meter (Model EA33, Extech Instruments, Waltham, MA), pressure chamber (Model 600, PMS Instruments, Corvallis, OR), and leaf porometer (Model SC-1, Decagon Devices, Pullman, WA), respectively. Light and g_s were measured at midday and Ψ was measured at predawn (Ψ_{PD}, the highest daily water status) and at midday (Ψ_{MD}, the lowest daily water status). For Ψ and g_s, three measurements were taken on three separate leaves and then averaged into a single value for that position. For g_s measurements, multiple readings were taken as needed until three values within 50 mmol H_2O m^{-2} s^{-1} of one another were attained and then averaged into a single value. For light, a measurement was

taken by each leaf for which g_s was measured; these light values were then averaged into a single value for that position.

Statistical Analyses

All statistical analyses were done using JMP (SAS Institute, Cary, NC). For categorical analyses comparing the response variables (LMA, A_{max}, A_{std}, R_{dark}, LSP, LCP, g_i, Ψ, g_s) among within-crown positions, one- and two-way ANOVAs were conducted using height, lateral position, and sampling date as effects. Shapiro-Wilk goodness of fit tests were used to test the assumption that data were normally distributed within groups; if this assumption was violated, Kruskal-Wallis tests were used to detect significant differences among groups. Levine and Bartlett tests were used to test the assumption of equal variance among groups; if this assumption was violated, Welch tests were used to detect significant differences among groups. If significant differences among groups were found, Tukey's HSD multiple means comparisons were used to determine how groups differed. Regression analyses along the vertical gradient were also performed for each of the response variables. For all statistical analyses, we used $\alpha = 0.05$.

Results

Leaf mass-to-area ratio increased with height and was generally higher in the outer crown compared to the inner crown (Figure 2A, Table 2). Both vertical ($P = 0.0002$) and lateral ($P = 0.0003$) positions were significant effects on LMA, and there was no significant interaction between these two effects ($P = 0.09$). We also found that LMA significantly increased with height ($P = 0.002$, $R^2 = 0.47$; Figure 2B).

Despite these positional differences in LMA, lab-based measurements under optimal conditions suggested minimal differences in leaf physiological capacity (Table 2). For photosynthetic capacity, area-based A_{std} was the only metric that significantly varied, with lateral position acting as a significant effect ($P = 0.04$), and there was a significant positive relationship between photosynthetic capacity and height ($P = 0.048$, $R^2 = 0.22$). The most notable trend measured was for area-based R_{dark} (Figure 2C), with vertical position acting as a significant effect ($P = 0.002$; Table 2) and a significant positive relationship with height ($P = 0.0001$, $R^2 = 0.61$; Figure 2D). We also found that LCP significantly varied, with vertical position acting as a significant effect ($P = 0.02$) and a significant positive relationship with height ($P = 0.03$, $R^2 = 0.25$; Table 2). The rest of the variables investigated (A_{max}, mass-based A_{std}, mass-based R_{dark}, g_i, and LSP) did not significantly vary among positions or with height under optimal lab-based conditions ($P > 0.05$; Table 2).

Although physiological capacity under optimal lab-based conditions was largely conserved across bigleaf maple leaf morphologies, our field-based findings indicate that different crown regions have notably different physiologies *in situ* when evaluating seasonal averages (Table 3). Light was a likely driver of these within-crown physiological trends, as height ($P = 0.004$) and lateral position ($P < 0.0001$) were both significant effects on light availability, and there was a significant interaction between these two effects ($P = 0.03$). As such, light was significantly higher in the outer mid-crown and outer treetop positions compared to all other positions ($P = 0.0003$; Figure 2E) and significantly increased with height ($P = 0.0001$, $R^2 = 0.36$; Figure 2F). Before sunrise, Ψ_{PD} did not vary with height ($P = 0.16$) or lateral position ($P = 0.64$), there was no interaction between these two effects ($P = 0.99$), and there was no significant relationship between Ψ_{PD} and height ($P = 0.38$, $R^2 = 0.02$). At midday, height ($P = 0.03$) had a significant effect on Ψ_{MD}, although lateral position ($P = 0.17$) and the interaction between these two positional effects ($P = 0.48$) were not significant (Table 3). Similar to the trends measured for Ψ_{PD}, we found no significant relationship between Ψ_{MD} and height ($P = 0.06$, $R^2 = 0.10$). At midday, g_s significantly varied with both height ($P = 0.0001$) and lateral position ($P < 0.0001$), and there was no interaction between the two effects ($P = 0.24$). As such, g_s was significantly higher in the treetop outer crown than in any other position ($P < 0.0001$; Figure 2G) and significantly increased with height ($P < 0.0001$, $R^2 = 0.39$; Figure 2H). These trends in g_s are likely explained by light availability ($P <$

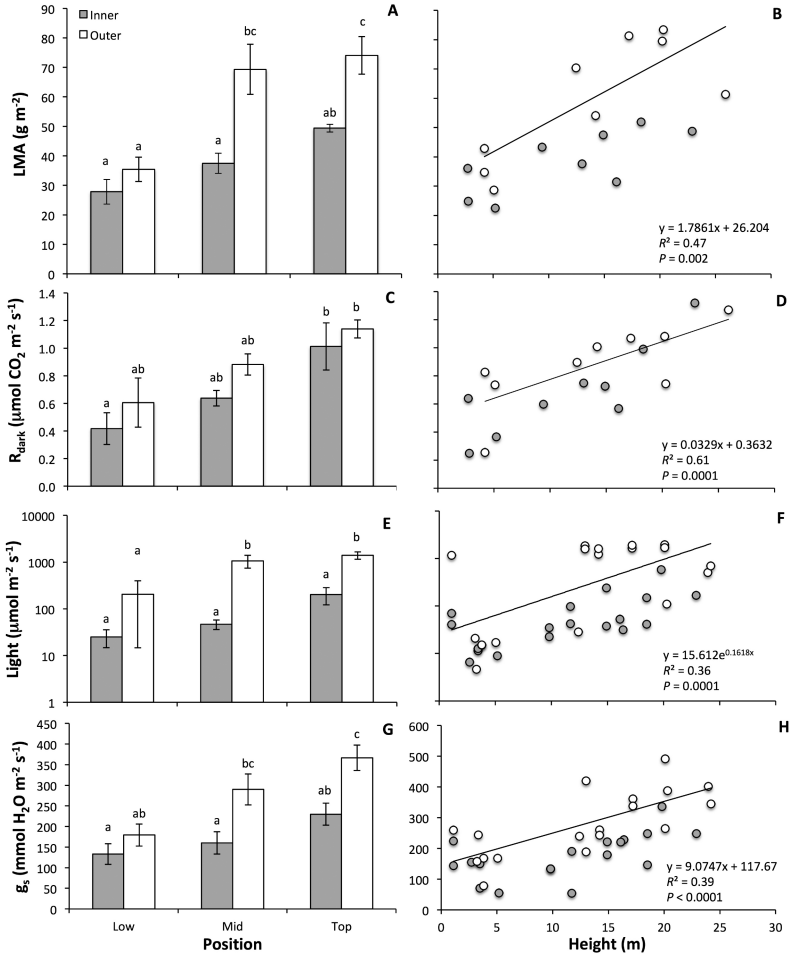

Figure 2. Bigleaf maple leaf characteristics for: leaf mass-to-area ratio (LMA) as related to vertical and lateral crown positions (A) and height (B); dark respiration rate (R_{dark}) on hydrated cuttings as related to vertical and lateral crown positions (C) and height (D); *in situ* light as related to vertical and lateral crown positions (E) and height (F); *in situ* stomatal conductance (g_s) as related to vertical and lateral crown positions (G) and height (H). Leaves were collected in 2016 in Maple Creek, CA at heights from the low-crown (4.0 ± 0.4 m), mid-crown (14.2 ± 1.5 m), and treetop (19.9 ± 1.6 m); for *in situ* data, measurements were taken across six sampling days between June and September. In column charts, columns represent means ± SE and positions not sharing the same letter are significantly different. Inner and outer crown positions represented by gray and white, respectively for all panels. For panels E and F, note the logarithmic scale on the vertical axes; for panels G and H, note the difference in scale between the vertical axes.

0.0001, $R^2 = 0.49$) and Ψ_{MD} ($P = 0.02$, $R^2 = 0.15$), as both variables were highly correlated with gas exchange rate (Figure 3).

A more fine-scale *in situ* investigation of maple crowns across the growing season showed striking temporal and spatial trends in light availability, Ψ, and g_s. On each sampling day between June and September, light availability generally increased with height and distance from the bole but did not markedly vary across the four months except for noticeably increasing in the mid- and low-crown in September (Figure 4A). Predawn Ψ was remarkably hydrated (always above -1 MPa) and constant among positions and sampling days across the growing season (Figure 4B). In contrast, Ψ_{MD} generally decreased with height and distance from the bole and also between June and September (Figure 4C). Following similar trends as light and Ψ_{MD}, g_s generally increased with height and distance from the bole. Notably, treetop g_s peaked in June, while mid-crown g_s peaked later in July and August, and low-crown g_s peaked at the end of the growing season in September (Figure 4D). These trends in g_s seem largely driven by light availability, as evidenced by the strong positive relationship between g_s and light (Figure 3A), and by the similarity of trends between g_s and light on all sampling days (Figures 4A, 4D). For example, when the low-crown experienced notably high light availability in September, this aligned with notably high g_s.

TABLE 2. Summary of morphology and gas exchange lab-based measurements (mean ± SE) on hydrated bigleaf maple cuttings from Maple Creek, CA in 2016. Cuttings were collected from inner and outer branch positions in the low-crown (4.0 ± 0.4 m), mid-crown (14.2 ± 1.5 m), and treetop (19.9 ± 1.6 m). Gas exchange rates reported on an area($_a$)- and a mass($_m$)-basis. Two-way ANOVA *P*-values provided for the significance of vertical and lateral positions as effects and the interaction between these two effects; as applicable, positions not sharing the same letter are significantly different. Regression statistics provided for each characteristic as it relates to height. Shaded cells indicate significance ($P \leq 0.05$). LMA = leaf mass-to-area ratio; A_{max} = maximum photosynthetic rate; A_{std} = standardized maximum photosynthetic rate; R_{dark} = dark respiration rate; g_i = internal CO_2 conductance rate; LSP = light saturation point; LCP = light compensation point.

Position (crown-branch)	LMA ($g\ m^{-2}$)	$A_{max,a}$ ($\mu mol\ CO_2\ m^{-2}\ s^{-1}$)	$A_{max,m}$ ($nmol\ CO_2\ g^{-1}\ s^{-1}$)	$A_{std,a}$ ($\mu mol\ CO_2\ m^{-2}\ s^{-1}$)	$A_{std,m}$ ($nmol\ CO_2\ g^{-1}\ s^{-1}$)	$R_{dark,a}$ ($\mu mol\ CO_2\ m^{-2}\ s^{-1}$)	$R_{dark,m}$ ($nmol\ CO_2\ g^{-1}\ s^{-1}$)	$g_{i,a}$ ($mol\ CO_2\ m^{-2}\ s^{-1}\ bar^{-1}$)	$g_{i,m}$ ($nmol\ CO_2\ g^{-1}\ s^{-1}\ bar^{-1}$)	LSP ($\mu mol\ m^{-2}\ s^{-1}$)	LCP ($\mu mol\ m^{-2}\ s^{-1}$)
Low-inner	28 ± 4^{a}	3.8 ± 0.8	147 ± 37	3.4 ± 0.4	127 ± 23	0.42 ± 0.12^{a}	15.7 ± 3.5	0.008 ± 0.002	0.32 ± 0.10	1072 ± 250	9 ± 3
Low-outer	35 ± 4^{a}	5.3 ± 1.2	144 ± 40	4.6 ± 0.8	118 ± 30	0.61 ± 0.18^{ab}	15.2 ± 4.2	0.020 ± 0.001	0.50 ± 0.04	1420 ± 328	21 ± 5
Mid-inner	37 ± 3^{a}	4.3 ± 0.8	112 ± 37	3.5 ± 0.3	87 ± 19	0.64 ± 0.06^{ab}	16.1 ± 2.1	0.017 ± 0.004	0.39 ± 0.07	1435 ± 392	16 ± 7
Mid-outer	69 ± 8^{bc}	9.7 ± 0.2	162 ± 30	8.3 ± 1.7	139 ± 24	0.88 ± 0.08^{ab}	14.9 ± 1.5	0.023 ± 0.007	0.38 ± 0.11	1544 ± 499	17 ± 4
Top-inner	49 ± 1^{ab}	5.7 ± 3.2	119 ± 66	5.0 ± 2.2	104 ± 47	1.01 ± 0.17^{b}	20.1 ± 3.5	0.010 ± 0.005	0.20 ± 0.11	1321 ± 452	33 ± 7
Top-outer	74 ± 6^{c}	6.1 ± 1.9	81 ± 24	6.2 ± 1.3	82 ± 19	1.14 ± 0.07^{b}	15.7 ± 1.7	0.040 ± 0.024	0.56 ± 0.35	1167 ± 144	29 ± 3
Vertical *P*	0.0002	0.44	0.52	0.32	0.41	0.002	0.63	0.70	0.98	0.75	0.02
Lateral *P*	0.0003	0.12	0.92	0.04	0.59	0.08	0.42	0.15	0.28	0.74	0.48
Vertical × Lateral *P*	0.09	0.39	0.57	0.30	0.76	0.89	0.79	0.58	0.58	0.79	0.41
Regression *P*	0.002	0.12	0.82	0.048	0.92	0.0001	0.23	0.09	0.41	0.19	0.03
Regression R^2	0.47	0.14	0.003	0.22	0.001	0.61	0.09	0.19	0.05	0.10	0.25

TABLE 3. Summary of *in situ* light and physiology field-based measurements (mean ± SE) in bigleaf maple trees from Maple Creek, CA. Measurements were taken from inner and outer branch positions at heights in the low-crown (4.0 ± 0.4 m), mid-crown (14.2 ± 1.5 m), and treetop (19.9 ± 1.6 m). Values represent means from across six sampling days in the 2016 growing season. Two-way ANOVA *P*-values provided for the significance of vertical and lateral positions as effects and the interaction between these two effects; as applicable, positions not sharing the same letter are significantly different. Regression statistics provided for each characteristic as it relates to height. Shaded cells indicate significance ($P \leq 0.05$); Ψ_{PD} = predawn water potential; Ψ_{MD} = midday water potential; g_s = stomatal conductance of water vapor.

Position (crown-branch)	Light (μmol m^{-2} s^{-1})	Ψ_{PD} (MPa)	Ψ_{MD} (MPa)	g_s (mmol H_2O m^{-2} s^{-1})
Low-inner	25 ± 10[a]	–0.50 ± 0.07	–0.87 ± 0.15	133 ± 25[a]
Low-outer	205 ± 191[a]	–0.52 ± 0.08	–0.85 ± 0.13	179 ± 27[ab]
Mid-inner	47 ± 11[a]	–0.58 ± 0.06	–1.00 ± 0.15	160 ± 27[a]
Mid-outer	1,067 ± 326[b]	–0.61 ± 0.07	–1.20 ± 0.21	290 ± 38[bc]
Top-inner	203 ± 82[a]	–0.62 ± 0.04	–1.12 ± 0.13	230 ± 27[ab]
Top-outer	1,398 ± 257[b]	–0.64 ± 0.05	–1.48 ± 0.15	367 ± 31[c]
Vertical *P*	0.004	0.16	0.03	0.0001
Lateral *P*	< 0.0001	0.64	0.17	< 0.0001
Vertical × Lateral *P*	0.03	0.99	0.48	0.24
Regression *P*	0.0001	0.38	0.06	< 0.0001
Regression R^2	0.36	0.02	0.10	0.39

Discussion

In contrast to tall conifers where the hydrostatic gradient can increase LMA and reduce photosynthetic capacity (Koch et al. 2004), in this shorter broadleaved species, the hydrostatic gradient does not appear to lower Ψ sufficiently to increase LMA. Our findings of a strong within-crown light gradient and consistently hydrated (above –2 MPa) Ψ_{MD} therefore suggest that light availability is the primary determinant of leaf morphology in bigleaf maple. In the low crown where inner and outer leaves were both shaded, LMA did not significantly differ between lateral positions. However, in the mid-crown and treetop, foliage had higher LMA in the outer sunlit positions compared to the inner shaded positions, demonstrating that bigleaf maple foliage has sufficient Ψ to allow structural plasticity in response to different light environments. This plasticity in the upper crown in response to light availability is in contrast to some tall conifers, where presumably the hydrostatic gradient limits foliar structural acclimation to light (Chin and Sillett 2019).

While we found significant differences in within-crown leaf morphology, physiological capacity under optimal conditions was surprisingly comparable among positions. Although the trend was not significant, we consistently observed the highest photosynthetic rates and light saturation points in outer leaves from the mid-crown. It appears that although LMA and presumably mesophyll density (Oldham et al. 2010) increased with height, this increase was not sufficient to limit g_i. Given that we detected within-crown variability in light and photosynthetic capacity, our measurements of stable LSP throughout crowns seem odd. However, LSP was also relatively conserved throughout large redwood crowns (Mullin et al. 2009), suggesting that variability in this characteristic may be unpredictable based on crown position. The most notable trend that we measured was an increase in area-based R_{dark} with height, although this increased leaf cost did not appear to predictably decrease photosynthetic capacity. Our measurements of increasing (albeit non-significantly) LCP with height was likely related to our observed trend of increasing respiratory cost with height. These lab-based findings under optimal conditions demonstrate that while bigleaf maple leaf structure has minimal influences on leaf physiology, there is some level of plasticity

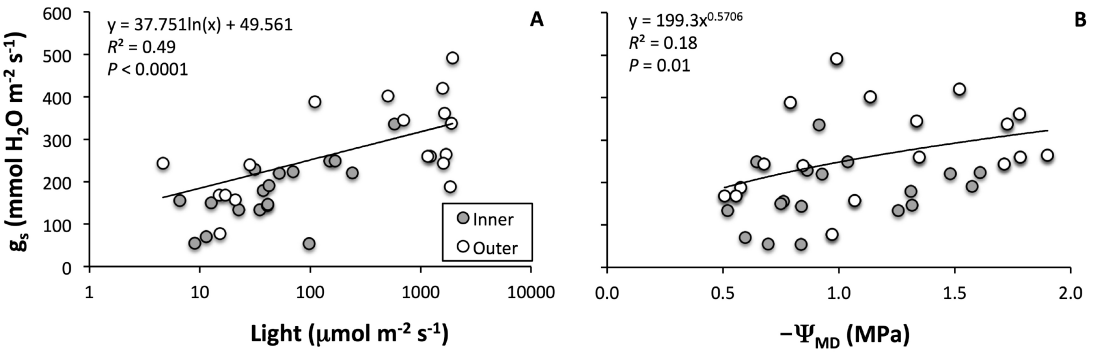

Figure 3. *In situ* stomatal conductance (g_s) as related to light (A) and midday water potential (Ψ_{MD}) (B) in bigleaf maple inner (gray) and outer (white) crowns. Measurements were taken across the 2016 growing season in Maple Creek, CA. Note the logarithmic scale on the horizontal axis of panel A.

in resource (e.g., nitrogen, chlorophyll, Rubisco) allocation to maximize photosynthetic capacity in high-light foliage.

Our *in situ* measurements across the growing season demonstrate compelling spatial and temporal trends in light availability, water status, and productivity (as inferred by g_s) in bigleaf maple trees. While light availability generally increased with height and distance from the bole, it was remarkably constant across time, except in September when there was a noticeable rise in low-crown light availability. We speculate that this rise in light availability in the low-crown is due to the onset of autumn leaf senescence in the treetop and mid-crown, allowing greater light penetration to deeper crown depths and also due to a lower angle of incoming solar radiation.

Similar to our measured trends in light availability, we found that water status was remarkably constant and hydrated throughout crowns and the growing season. Predawn Ψ is often thought of as a proxy for soil water potential, a measure of plant-available water. Our measurements of consistently high Ψ_{PD} across space and time indicate that soil water was sufficient to allow nightly rehydration. We note that 2016 was a moderately dry year, with a Palmer Drought Severity Index of –1.6 at this site (PRISM), and that perhaps in drier years, winter water inputs would begin to deplete later in the growing season and limit productivity. At midday, Ψ_{MD} generally decreased with height and distance from the bole, likely due to increased light increasing transpirational water loss. As such, water potential in the low crown decreased very little between predawn and midday, while in the mid-crown and treetop, there was a more marked decrease in Ψ between predawn and midday. This decrease was most pronounced in the outer leaves where we measured the greatest g_s. Across the growing season, Ψ_{MD} generally decreased, presumably due to increasing atmospheric VPD, but did not drop below –2 MPa. While these high Ψ_{MD} values suggest that either soil water was sufficient to keep trees relatively hydrated or that water potentials of roughly –2 MPa trigger stomatal regulation to conserve water, our data generally support the former possible explanation. Consistently high Ψ_{PD} measurements (generally above –0.75 MPa) indicate that ample soil water availability supported nightly whole-tree equilibration across the entire growing season. That g_s increased as Ψ_{MD} decreased suggests that Ψ_{MD} did not reach values low enough to stimulate stomatal closure. Regardless of the mechanism(s) (sufficient soil water and/or stomatal regulation), our high Ψ_{MD} measurements suggest that water availability did not limit bigleaf maple gas exchange.

As such, we found that g_s generally increased with height and distance from the bole, a spatial trend likely attributable to increased light availability coupled with negligible hydrostatic constraints. Because maple wood can be relatively

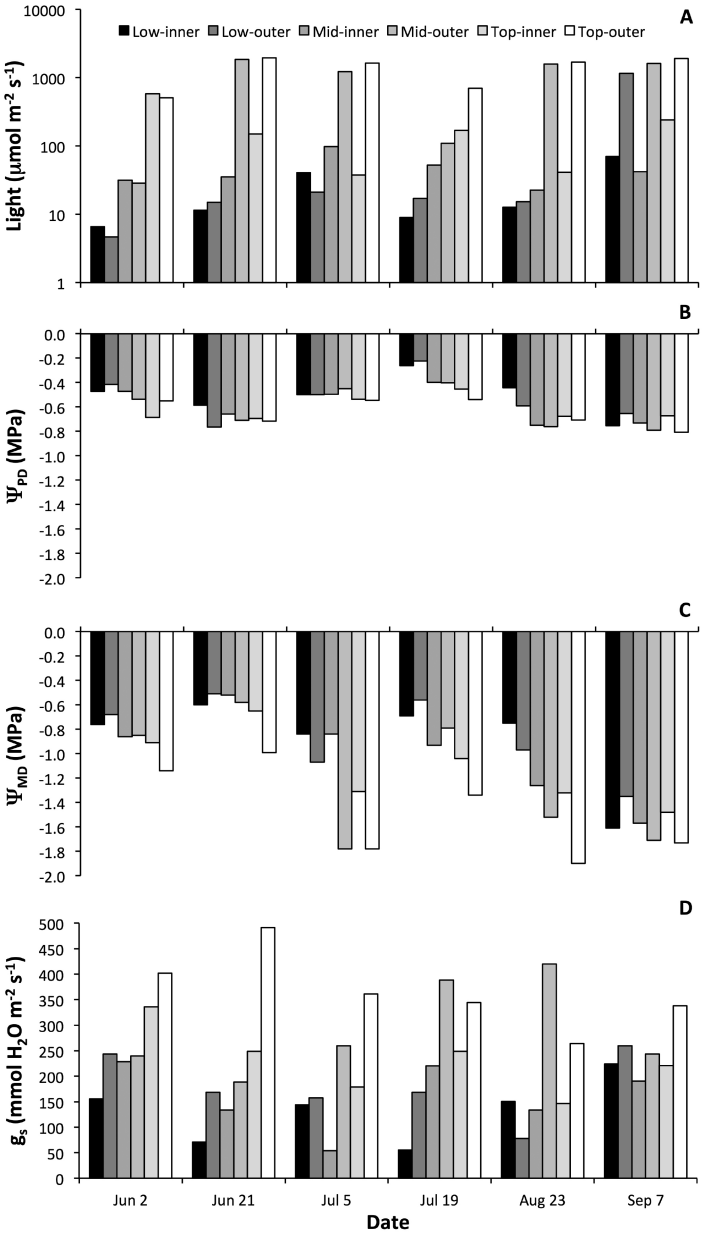

Figure 4. *In situ* measurements of (A) light, (B) predawn water potential (Ψ_{PD}), (C) midday water potential (Ψ_{MD}), and (D) stomatal conductance (g_s) as categorically related to vertical and lateral crown positions. Measurements were taken in bigleaf maple trees in 2016 in Maple Creek, CA from the low-crown (4.0 ± 0.4 m), mid-crown (14.2 ± 1.5 m), and treetop (19.9 ± 1.6 m). Each column represents the mean of three measurements taken in one tree.

resistant to cavitation, only losing 50% of hydraulic capacity at a water potential of –5 MPa (Taneda and Sperry 2008), some maple species are able to maintain stomatal conductance despite decreasing water potential. We speculate that as bigleaf maples typically only grow to be roughly 30 m tall and likely can withstand low Ψ values without experiencing cavitation, gas exchange is not likely hydraulically limited in the upper crowns by gravity and transpirational friction, as seen in taller trees (Couvreur et al. 2018).

Temporally, we found that g_s peaked relatively early (June) in treetops, slightly later (July and August) in mid-crowns, and relatively late (September) in low-crowns. We speculate that this wave of maximum seasonal g_s shifting from the treetop to the low-crown across time is likely due to the shifting angle of incoming sunlight across the growing season, boosting g_s in different crown locations, with June light targeting treetops, July/August light targeting mid-crowns, and September light targeting low-crowns. Alternatively, our observed trends in g_s could be due to the onset of leaf senescence slowing gas exchange in the upper crown and allowing greater light penetration to the lower crown. Finally, this spatial and temporal shift in maximum g_s could be driven by stomatal regulation at low Ψ_{MD} values limiting g_s from the treetop downward as the season progresses. This latter explanation makes sense, as treetops would be the first to reach low

Ψ_{MD} values due to greater exposure to light and wind increasing transpirational water loss and due to greater (although still relatively minimal) hydrostatic constraints. Although this final explanation for g_s trends is theoretically possible, the fact that *in situ* g_s increased with decreasing Ψ_{MD} suggests that water status did not limit gas exchange. Regardless of the mechanism(s), these g_s trends demonstrate a shifting optimization of crown resources to maximize whole-tree carbon uptake across space and time.

This study used lab- and field-based measurements to quantify spatial and temporal trends in leaf morphology and physiology within bigleaf maple crowns. We found that LMA increased with height and distance from the bole and that this morphological variation affected leaf physiology such that outer mid-crown foliage had the highest photosynthetic capacity. Within crowns, we measured increasing light availability with height and distance from the bole, and therefore attribute much of our observed variation in leaf morphology and physiology to differences in light environment. We consistently measured high Ψ within crowns across the growing season, indicating that there is sufficient residual soil water from winter rain deposits and/or that this species uses stomatal regulation to limit water loss. *In situ*, we found that productivity (as measured by g_s) increased with height and distance from the bole, peaked at different times throughout the growing season in different crown positions, was positively correlated with light availability, and could possibly be limited by stomatal regulation late in the season under elevated midday temperatures and VPD. Due to inherently higher photosynthetic capacity related to leaf structure and *in situ* higher light availability and minimal hydraulic limitation, upper crowns seem to have the highest productivity within bigleaf maple trees. For next steps to improve understanding of hardwood seasonal physiology and productivity, it would be informative to quantify if/how these trends vary between relatively dry and wet years, as this information would help refine our understanding of forest responses to a changing climate.

Acknowledgments

We thank the L.W. Schatz Demonstration Tree Farm and the Humboldt State University Department of Forestry and Wildland Resources for access to this study site and financial support of this project. We are grateful to Wade Polda, Gabriel Goff, and Nicholas Kilgore for assistance with fieldwork, and Ariel Weisgrau for assistance with lab measurements. We also thank Shan Kothari and one anonymous reviewer for helpful comments that improved this manuscript.

Literature Cited

Catoni, R., L. Gratani, F. Sartori, L. Varone, and M. U. Granata. 2015. Carbon gain optimization in five broadleaf deciduous trees in response to light variation within the crown: correlations among morphological, anatomical and physiological leaf traits. Acta Botanica Croatica 74:71-94.

Chin, A. R. O., and S. C. Sillett. 2017. Leaf acclimation to light availability supports rapid growth in tall *Picea sitchensis* trees. Tree Physiology 37:1352-1366.

Chin, A. R. O., and S. C. Sillett. 2019. Within-crown plasticity in leaf traits among the tallest conifers. American Journal of Botany 30:1-13.

Couvreur, V., G. Ledder, S. Manzoni, D. A. Way, E. B. Muller, and S. E. Russo. 2018. Water transport through tall trees: A vertically explicit, analytical model of xylem hydraulic conductance in stems. Plant Cell and Environment 41:1821-1839.

Davies, W. J., and T. Kozlowski. 1977. Variations among woody plants in stomatal conductance and photosynthesis during and after drought. Plant and Soil 46:435-444.

Ingraham, N. L., and R. A. Matthews. 1995. The importance of fog-drip water to vegetation: Point Reyes Peninsula, California. Journal of Hydrology 164:269-285.

Kerhoulas, L. P., A. S. Weisgrau, E. C. Hoeft, and N. J. Kerhoulas. 2020. Vertical gradients in foliar physiology of tall *Picea sitchensis* trees. Tree Physiology 40:321-332.

Koch, G. W., S. C. Sillett, G. Jennings, and S. Davis. 2004. The limits to tree height. Nature 428:851-854.

Kramer, R. D., S. C. Sillett, and R. Van Pelt. 2018. Quantifying aboveground components of *Picea sitchensis* for allometric comparisons among tall conifers in North American rainforests. Forest Ecology and Management 430:59-77.

Lichtenthaler, H. K., C. Buschmann, M. Döll, H. J. Fietz, T. Bach, U. Kozel, D. Meier, and U. Rahmsdorf. 1981. Photosynthetic activity, chloroplast ultrastructure, and leaf characteristics of high-light and low-light plants and of sun and shade leaves. Photosynthesis Research 2:115-141.

Mullin, L. P., S. C. Sillett, G. W. Koch, K. P. Tu, and M. E. Antoine. 2009. Physiological consequences of height-related morphological variation in *Sequoia sempervirens* foliage. Tree Physiology 29:999-1010.

Oldham, A. R., S. C. Sillett, A. M. F. Tomescu, and G. W. Koch. 2010. The hydrostatic gradient, not light availability, drives height-related variation in *Sequoia sempervirens* (Cupressaceae) leaf anatomy. American Journal of Botany 97:1087-1098.

Rhemtulla, J. M., D. J. Mladenoff, and M. K. Clayton. 2009. Historical forest baselines reveal potential for continued carbon sequestration. Proceedings of the National Academy of Sciences 106:6082-6087.

Sohngen, B., and S. Brown. 2006. The influence of conversion of forest types on carbon sequestration and other ecosystem services in the South Central United States. Ecological Economics 57:698-708.

Stone, E. L., and P. J. Kalisz. 1991. On the maximum extent of tree roots. Forest Ecology and Management 46:59-102.

Stuart, J. D., and J. O. Sawyer. 2001. Trees and Shrubs of California. University of California Press, Berkeley.

Taneda, H., and J. Sperry. 2008. A case-study of water transport in co-occurring ring-versus diffuse-porous trees: contrasts in water-status, conducting capacity, cavitation and vessel refilling. Tree Physiology 28:1641-1651.

Weatherbase National Database. 2019. Maple Creek, California. Canty and Associates LLC, Great Falls, VA. Available online at https://www.weatherbase.com/weather/weather-summary.php3?s=332140&cityname=Maple+creek%2C+California%2C+United+States+of+America&units (accessed 30 April 2019).

Woodruff, D. R., B. J. Bond, and F. C. Meinzer. 2004. Does turgor limit growth in tall trees? Plant, Cell and Environment 27:229-236.

Received 03 October 2019
Accepted 13 March 2020